Journal of Power Sources 233 (2013) 277–284

Contents lists available at SciVerse ScienceDirect

Journal of Power Sources

journal homepage: www.elsevier.com/locate/jpowsour

A new method to estimate the state of charge of lithium-ion batteries based on the battery impedance model

Jun Xu [a,b], Chunting Chris Mi [b,*], Binggang Cao [a], Junyi Cao [a]

[a] Xi'an Jiaotong University, Xi'an, Shannxi, 710049, China
[b] University of Michigan-Dearborn, Dearborn, MI 48188, USA

HIGHLIGHTS

- Derived a simplified lithium ion battery impedance model based on impedance spectra.
- The model can maintain accuracy but is more concise and easier to implement.
- Fractional modeling method is introduced to model the CPE of the impedance model.
- Proposed a new method to identify the impedance model.
- Fractional Kalman filter is introduced to estimate the states such as SOC.

ARTICLE INFO

Article history:
Received 17 July 2012
Received in revised form
29 November 2012
Accepted 16 January 2013
Available online 24 January 2013

Keywords:
Lithium ion battery
Electric vehicle
State of charge
Impedance model
Fractional Kalman filter
Fractional order calculus (FOC)

ABSTRACT

This paper deals with the problem of estimating the state of charge (SOC) of lithium-ion batteries. Based on the analysis of the impedance spectra obtained by electrochemical impedance spectroscopy (EIS), a simplified battery impedance model is derived with the constant phase element (CPE). To interpret the impedance model, a fractional order calculus (FOC) method is introduced to model the CPE in the impedance model. A new identification method is proposed to identify the impedance model, considering both accuracy and simplicity. The fractional Kalman filter is introduced to estimate the SOC of the lithium-ion battery based on the impedance model. Finally, a battery test bench is established, and the proposed method is verified by a scaled down system on the urban dynamometer driving schedule (UDDS) drive cycle test.

1. Introduction

With the development of Electric Drive Vehicles (EDVs), including Battery Electric Vehicle (BEV), Hybrid Electric Vehicle (HEV), and Plug-in Hybrid Electric Vehicle (PHEV), battery technology has drawn more and more attention worldwide. Moreover, based on the exiting battery technology, one key research area in batteries is to improve the utilization rate and the life of the battery used in EDVs. Considered as the only viable solution for EDVs at the present time, lithium-ion (Li-ion) batteries should not be overcharged or over-discharged to avoid damage of the battery, shortening the battery life, fire or explosions. The accuracy of battery state of charge (SOC) is one of the key points to avoid overcharging and over-discharging. Meanwhile, an accurate SOC could also lead to a more accurate estimation of the drive distance of an EDV.

The definition of SOC is the ratio of the remaining capacity to the nominal capacity of the battery, which can be described as:

$$\mathrm{SOC} = \frac{\text{Remaining Capacity}}{\text{Norminal Capacity}} \tag{1}$$

If an accurate SOC can be obtained, the useable SOC range could be extended. Thus, a smaller battery pack would be able to satisfy the demand of an EV that right now is equipped with a larger battery pack. Thus the price for the battery pack could be dramatically decreased, further helping the market penetration of EDVs.

* Corresponding author. Tel.: +1 313 583 6434; fax: +1 313 583 6336.
E-mail address: chrismi@umich.edu (C.C. Mi).

0378-7753/$ – see front matter © 2013 Elsevier B.V. All rights reserved.
http://dx.doi.org/10.1016/j.jpowsour.2013.01.094

The battery is an electrochemical system with strong nonlinearity. To model such a strong nonlinear system is very difficult. To draw states that cannot be measured directly, such as the SOC and parameters of a battery, will be even more difficult.

The ampere-hour counting (Coulomb counting, or current integration) method for the calculation of battery SOC is simple and easy to implement, but the method needs the prior knowledge of initial SOC and suffers from accumulated errors from noise and measurement error. The open-circuit voltage (OCV) method is very accurate, but this method needs a long rest time to estimate the SOC and thus cannot be used in real time. SOC estimation method based on an accurate battery model is the most popular solution. Some attempts have been made to evaluate the models for the state and parameter estimation of a Li-ion battery, such as the Rin Model [1–3], the first order RC model [3–5], the second order RC model [3,6], etc. More models have also been researched derived from the models mentioned above, such as hysteresis model [1]. Normally, the estimation will be more accurate if the model can characterize the battery better. The models mentioned above are widely used but not good enough to get satisfying estimation results.

The Electrochemical Impedance Spectroscopy (EIS) method is considered one of the most accurate methods to model an electrochemical system, including Li-ion batteries [7–9]. However, studies have shown that the EIS method is too complex to be implemented in real time applications [10]. There are many studies which tried to utilize the impedance spectra directly to estimate SOC. Researchers tried to look for possible correlations between certain electrical parameters derived from experimental impedance spectra and SOC, only to find that there is no clear cut dependency on SOC [11]. The impedance spectra vary with temperature, which adds difficulty to derive SOC directly from the impedance spectra.

The main purpose of this paper is to take advantage of the accuracy of EIS properties, and derive an impedance model from the impedance spectra. It then focuses on finding an approach to estimate the SOC of a battery based on the impedance model.

A fractional order calculus (FOC) method is introduced to solve the problem. FOC is a natural extension of the classical integral order calculus. Studies have indicated that most phenomena, such as viscoelasticity, damp, fluid, friction, chaos, mechanical vibration, dynamic backlash, sound diffusion, etc, have fractional properties [12,13]. Furthermore, Machado pointed out that the entire system had fractional properties, even if parts of it had integral properties [14]. Thus, FOC is widely used in modeling, control, signal processing, etc. [12,15,16]. More and more researches have been carried out based on FOC to develop electrochemical models [17,18], including supercapacitors, lead-acid batteries, Li-ion batteries, fuel cells and so on.

A fractional modeling method is utilized to interpret the impedance model, so that the impedance model can be represented in equations and become more convenient to implement the SOC estimation of a battery. To take advantage of Kalman filter, popularly used in estimation problems, and considering the properties of the impedance model, the traditional Kalman filter is modified and the fractional Kalman filter is introduced to estimate the SOC based on the impedance model.

2. Impedance analysis and modeling

EIS is an experimental method to characterize electrochemical systems, such as batteries, supercapacitors, etc. During the measurement of an EIS, a small AC current flows through the battery and the voltage, the response with respect to amplitude and phase, is measured. The impedance of the system is determined by the complex division of AC voltage by AC current. This sequence is repeated for a certain range of different frequencies, and the full range of frequency properties of the battery could be obtained [19]. EIS gives a precise impedance measurement in a wide band of frequencies, thus provides a unique tool for analysis of the dynamical behavior of batteries, which measures the nonlinearities as well as very slow dynamics directly.

Fig. 1 shows the impedance spectra of the Li-ion battery at 50% SOC and measured over frequencies ranging from 3 MHz to 2.1 kHz. As shown in the figure, the impedance spectra can be divided into three sections: the high-frequency section, the mid-frequency section and the low-frequency section [19].

In the high-frequency section (>144 Hz), the impedance spectra intersect with the real axis and the point could be represented by an Ohmic resistance.

In the low-frequency section (<443 mHz), the curve is a straight line with a constant slope, which means that the low-frequency section could be expressed as a constant phase element (CPE) [9,17,20], usually referred to as a Warburg element. The equation of a Warburg element is listed as:

$$Z_{\text{warburg}}(j\omega) = \sqrt{\frac{R_D}{j\omega C_D}}\cdot\coth\left(\sqrt{R_D\cdot j\omega C_D}\right) \tag{2}$$

The mid-frequency section (443 mHz - 144 Hz) forms a depressed semicircle, which is a well-known phenomenon in electrochemistry [20]. Such a depressed semicircle could be modeled by paralleling a CPE with a resistance, which is referred to as a ZARC element. From the analysis above, the equivalent circuit is depicted as shown in Fig. 2.

In Fig. 2, V_{ocv} denotes the open circuit voltage of the battery; V_1, V_2, and V_3 denote the voltage for R_1, ZARC and Warburg respectively; V_o is the voltage output of the battery which can be measured directly from the two terminals of the battery. The current is assumed to be positive when the battery discharges and negative when the battery charges. Now, how does one use such an impedance model with CPE?

A FOC modeling method is introduced to interpret such an element. A fractional element is given as [12]:

$$Z_{\text{fractional}}(j\omega) = \frac{1}{Q(j\omega)^r} \tag{3}$$

where $Q \in R$ is the coefficient; $r \in R\,(-1 \le r \le 1)$ is the arbitrary order of the fractional element, which can be an integer or a fraction. In the case $r = 0$, the fractional element is equivalent to a resistor; in

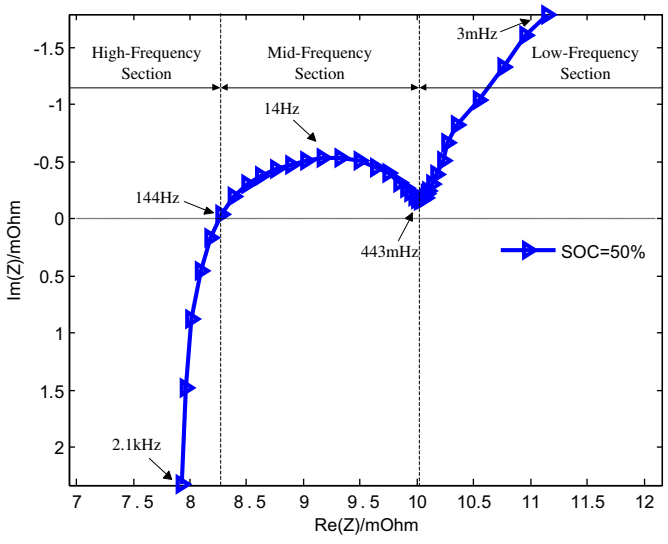

Fig. 1. Impedance spectra of a Li-ion battery.

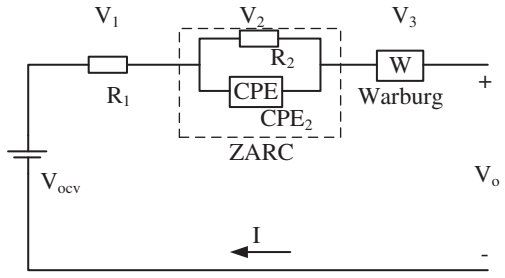

Fig. 2. Equivalent circuit of the impedance model.

the case $r = 1$, it is equivalent to a capacitor; in the case $r = -1$, it is equivalent to an inductor.

Furthermore, the magnitude of the fractional element listed in (3) is 20r dB dec-1, the phase is $r\pi/2$, and the curve in Nyquist plot is a straight line with constant slope of $r\pi/2$. From the discussion above, it is effective to express a CPE with a fractional element, which is also proved in Ref. [12]. So, a Warburg element can be modeled by a fractional element $Z_{warburgf}$ as shown in (4), and the slope of the curve in the low-frequency section can be used to determine the parameter r, which will be discussed in detail in the next section. A Warburg element can be expressed in terms of a fractional element as follow:

$$Z_{\text{warburgf}}(j\omega) = \frac{1}{W(j\omega)^{\alpha}} \tag{4}$$

where $\alpha \in R$, $0 \le \alpha \le 1$ is an arbitrary number, $W \in R$ is the coefficient.

Similarly, assume the equation of CPE_2 as follows:

$$Z_{\text{CPE}_2}(j\omega) = \frac{1}{C_2(j\omega)^{\beta}} \tag{5}$$

where $\beta \in R, 0 \le \beta \le 1$ is an arbitrary number, and $C_2 \in R$ is the coefficient, especially, when $\beta = 1$,

$$Z_{\text{CPE}_2}(j\omega)|_{\beta=1} = \frac{1}{C_2(j\omega)} \tag{6}$$

At this time, CPE_2 is a capacitor with capacitance C_2, and the Nyquist plot of the paralleling CPE and resistor is a semicircle.

Fig. 3 depicts the results when $Z_{warburgf}$ is used instead of $Z_{warburg}$ and ZARC is represented by FOC in the impedance model.

Fig. 3 shows that the proposed method can fit the measured impedance spectra well. This means that the impedance model can characterize the Li-ion battery well and the FOC can interpret the impedance model well.

For the sake of simplification, the equation below defines the denotation of the FOC [13]

$${}_a\Delta_t^r = \begin{cases} \dfrac{\mathrm{d}^{\mathrm{r}}}{\mathrm{d}t^{\mathrm{r}}} & : r > 0, \\ 1 & : r = 0, \\ \displaystyle\int_a^t (\mathrm{d}\tau)^{-\mathrm{r}} & : r < 0. \end{cases} \tag{7}$$

where $r \in R$ is an arbitrary number. It is considered to be in the condition $r \ge 0$ in this paper, which means the FOC in this paper is always a fractional differentiation, so ${}_a\Delta_t^r$ is simplified as Δ^r.

From the equivalent circuit illustrated in Fig. 2 and the analysis shown above, according to the circuit theory, the equations can be obtained as follows:

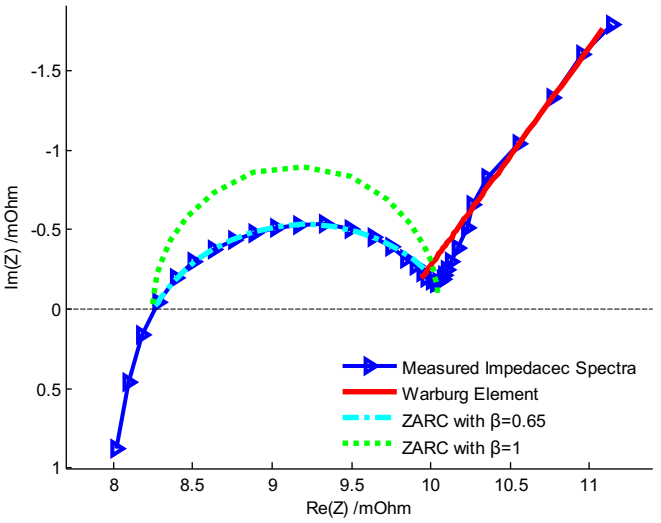

Fig. 3. Comparison between measured impedance spectra and the impedance model.

$$-I = C_2 \cdot \Delta^{\beta} V_2 + \frac{V_2}{R_2} \tag{8}$$

So

$$\Delta^{\beta} V_2 = -\frac{1}{R_2 C_2} \cdot V_2 - \frac{1}{C_2} \cdot I \tag{9}$$

From (4), the Warburg element can be rewritten as follows:

$$\Delta^{\alpha} V_3 = -\frac{1}{W} \cdot I \tag{10}$$

For the whole circuit shown in Fig. 2, the following relationship can be obtained:

$$V_o = V_{ocv} + V_1 + V_2 + V_3 = V_{ocv} + V_2 + V_3 - R_1 \cdot I \tag{11}$$

These equations could be alternated as follows:

$$\begin{cases} \Delta^N x = A \cdot x + B \cdot I \\ y = C \cdot x + D \cdot I \end{cases} \tag{12}$$

where: $A = \begin{bmatrix} -1/R_2C_2 & 0 \\ 0 & 0 \end{bmatrix}$, $B = \begin{bmatrix} -1/C_2 \\ -1/W \end{bmatrix}$, $N = \begin{bmatrix} \beta \\ \alpha \end{bmatrix}$, $C = [1 \quad 1]$, $D = -R_1$, $y = V_o - V_{ocv}$, $x \in R^2$ is the system state vector and the first equation of (12) is called the state space function, which captures the system dynamics. $y \in R$ as the output of the system is a combination of states x and input vector $I \in R$.

3. Identification of the impedance model

Based on the analysis of impedance spectra and the properties of FOC, a new identification method is proposed. The order of the Warburg element is identified from the impedance spectra. Based on the structure of the impedance model and the parameter identified from the impedance spectra, the least-square method is utilized to identify the remaining parameters in the time domain with the voltage response of the battery.

As depicted in Fig. 1, the low-frequency section of the impedance spectra is a straight line with a constant slope. Fig. 4 shows the impedance spectra of the battery in different SOC states, which shows that the curvatures of the impedance spectra are almost the same. The low-frequency section curves almost overlap each other, which means the straight lines of the different SOC impedance

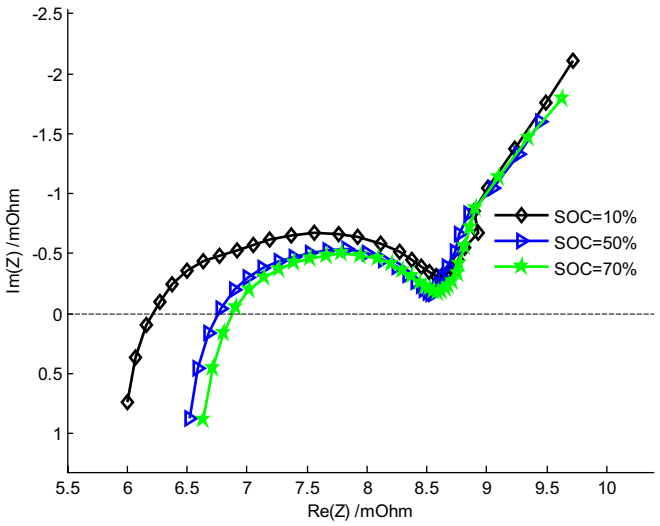

Fig. 4. Impedance spectra in different SOC state.

spectra share the same slope. This Warburg element is expressed by a fractional element shown in (4), which has the slope of $\alpha\pi/2$. So parameter α is easily obtained from the low-frequency section impedance spectra. Since the slope of the low-frequency section impedance spectra is nearly the same in different SOC conditions, that is $\pi/4$, α can be identified as 0.5 for different SOC.

However, impedance spectra are not easy to obtain, especially in real time applications. A voltage response of the battery is studied in Fig. 5. The voltage response curve can be divided into three sections, response from R1, response from ZARC and response from Warburg, which coincide with the impedance model. The least square method is utilized to identify the remaining parameters according to the voltage response shown in Fig. 5.

To show the superiority of the impedance model, a popular first order RC model (called RC model in this paper) is compared to the proposed impedance model. The procedure of the identification of the RC model is the same as that of the impedance model in the time domain. The same least square method is also applied to the RC model. The identification results are listed in Table 1. It can be seen from Table 1 that the root mean square (RMS) errors of impedance model are much smaller than that of the RC model, in any range of SOC. The mean percentage of impedance model RMS errors dividing by RC model RMS errors is about 50%. This means

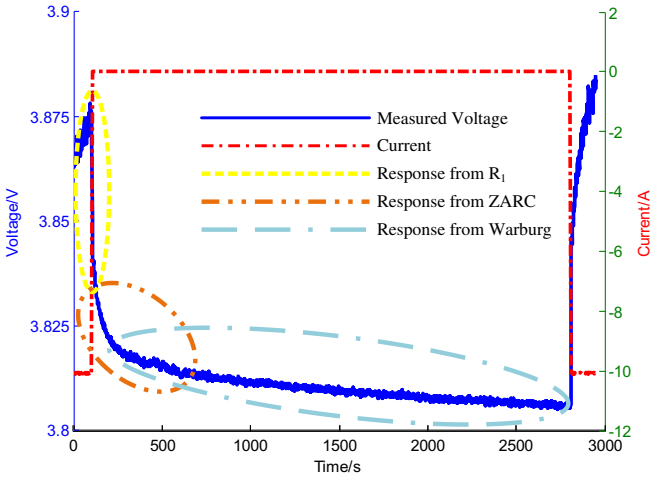

Fig. 5. Interpretation of the voltage response.

that the impedance model characterizes the Li-ion battery much better than the RC model does.

An urban dynamometer driving schedule (UDDS) drive cycle is used to verify the impedance model. The procedure is given in the experiment section. Fig. 6 shows the results of the verification and the comparison with the RC model. In Fig. 6, the RC model is referred to as RC and the impedance model is referred to as IM. An agreement between the simulated and the measured battery behavior has been demonstrated in Fig. 6. It indicates that the impedance model can characterize the properties of the battery quite well.

The impedance model is presented in an equivalent circuit with two CPE. With the development of FOC, such CPE, which in this paper is equivalent to a fractional element, can be easily realized with equivalent circuits with resistors and capacitors [12]. Thus, the impedance model is quit suitable to be introduced to EV/HEV real time simulation. However, such works are out the scope of this paper so they are not included.

4. Estimation based on the impedance model

Model based estimation theory is utilized in this paper to estimate the SOC of the Li-ion battery. A model of the battery dynamics and an algorithm that uses that model is needed to implement the model based estimation. The main methodology uses the input signals to run through the model and calculate the output from the model using the present and/or past states and parameters of the model. The difference between the calculated value and the measured values can be contributed to errors in the measurement, states, and parameters. Such differences or so-called errors are applied to an algorithm to intelligently update the estimation of the model states.

The Kalman filter is one of such algorithms, which are widely used. If the wanted unknown quantities are modeled in the state functions of the model, then a Kalman filter could be used to estimate such values. Since the impedance model derived in this paper is hard to implement with the CPE in the model, the traditional Kalman filter is not suitable for such a model. As discussed in Section 1, the CPE could be interpreted by FOC, to estimate the SOC of the battery based on the impedance model introduced in this paper, a fractional Kalman filter [21] is introduced to solve the problem.

The states used in the estimation method should be discussed first. In most studies, the OCV is estimated based on a model based method, and SOC is inferred from the OCV. In this paper, SOC is chosen as a state instead of OCV. The relationship between SOC and OCV is nonlinear and it is not easy to draw a mathematical interpretation for it. In dealing with this problem, a gain scheduling method [22] is introduced, which typically employs an approach whereby the nonlinear system is decomposed into a number of liner subsystems. For a given nonlinear system, the relationship between SOC and OCV can be divided into several sections, and the subsystem in each section is considered to be linear as shown in Fig. 7.

So the relationship can be written in the short SOC interval as follows:

$$V_{\mathrm{ocv}} = k_i \cdot \mathrm{SOC_i} + b_i \tag{13}$$

for the ith SOC interval $(i-1)\cdot\Delta_{\mathrm{soc}} \le \mathrm{SOC_i} \le i\cdot\Delta_{\mathrm{soc}}$, where Δ_{soc} is the SOC interval length. For the ith SOC interval $(i-1)\cdot\Delta_{\mathrm{soc}} \le \mathrm{SOC_i} \le i\cdot\Delta_{\mathrm{soc}}$, the corresponding set (k_i, b_i) can be calculated from the curve and will maintain constant in the ith SOC interval. The parameters of the approximation of the relationship between SOC and OCV are listed in Table 2. The measured and approximated curves of the relationship between SOC and OCV are shown in Fig. 7. The two curves are very consistent, indicating that such an approximation is reasonable and has sufficient accuracy.

Table 1
RMS errors of the identification results.

SOC/%	10–20	20–30	30–40	40–50	50–60	60–70	70–80	80–90
Impedance model (Charge)/V	0.125	0.083	0.099	0.145	0.186	0.088	0.091	0.110
RC model (Charge)/V	0.200	0.140	0.181	0.275	0.268	0.133	0.134	0.187
Impedance model (Discharge)/V	0.268	0.126	0.087	0.037	0.070	0.075	0.118	0.158
RC model (Discharge)/V	0.423	0.262	0.173	0.283	0.537	0.126	0.161	0.316

According to the explanation above, the state space function with the additional state SOC can be rewritten as:

$$\begin{cases} \Delta^{\beta} V_2 = -\dfrac{1}{R_2 C_2}\cdot V_2 - \dfrac{1}{C_2}\cdot I \\ \Delta^{\alpha} V_3 = -\dfrac{1}{W}\cdot I \\ \Delta^{1} z = -\dfrac{1}{C_n}\cdot I \end{cases} \tag{14}$$

$$V_o = V_2 + V_3 + k_i\cdot z + b_i - R_1\cdot I \tag{15}$$

where V_o is the output voltage of the battery, z denotes the SOC and T_s is the sample time, which is selected as 0.1 s in this paper.

It can be rewritten as follows in state space function form:

$$\begin{cases} \Delta^N x = A\cdot x + B\cdot I \\ y = C\cdot x + D\cdot I \end{cases} \tag{16}$$

where: $x = \begin{bmatrix} V_2 \\ V_3 \\ z \end{bmatrix}$, $A = \begin{bmatrix} -1/R_2C_2 & 0 & 0 \\ 0 & 0 & 0 \\ 0 & 0 & 0 \end{bmatrix}$, $B = \begin{bmatrix} -1/C_2 \\ -1/W \\ -1/C_n \end{bmatrix}$,

$N = \begin{bmatrix} \beta \\ \alpha \\ 1 \end{bmatrix}$, $C = [1 \quad 1 \quad k_i]$, $D = -R_1$, $y = V_o - b_i$.

According to (16) and the stochastic theory, the discrete state space function is obtained:

$$\begin{cases} \Delta^N x_{k+1} = A\cdot x_k + B\cdot I_k + \omega_k \\ y_k = C\cdot x_k + D\cdot I_k + v_k \end{cases} \tag{17}$$

where, at time index k, $x_k \in R^3$ is the state vector; $I_k \in R$ is the system input; $y_k \in R$ is the system output; $\omega_k \in R^3$ stochastic "process noise" or "disturbance" that models some unmeasured input, which affects the state of the system; $v_k \in R$ is the output noise. ω_k and v_k are assumed to be independent, zero mean Gaussian noise processes of the convariance matrices Q_k and R_k respectively.

To form the recursive algorithm, the relationship between x_{k+1} and x_k is needed, so according to (17), $\Delta^N x_{k+1}$ should be represented in the form of x_{k+1}. The fractional order Grünwald–Letnikov definition is given as [12]:

$$\Delta^{N} x_k = \frac{1}{T_s^N}\sum_{j=0}^{k}(-1)^j \binom{N}{j} x_{k-j} \tag{18}$$

where T_s is the sample interval, k is the number of samples for which the derivative is calculated, $\binom{N}{j} = \begin{cases} 1 & \text{for } j = 0, \\ N(N-1)\cdots(N-j+1)/j! & \text{for } j > 0. \end{cases}$

According to the definition of FOC

$$\begin{aligned} \Delta^N x_{k+1} &= \frac{1}{T_s^N}\sum_{j=0}^{k+1}(-1)^j \binom{N}{j} x_{k+1-j} \\ &= \frac{1}{T_s^N}(-1)^0 \binom{N}{0} x_{k+1-0} + \frac{1}{T_s^N}\sum_{j=1}^{k+1}(-1)^j \binom{N}{j} x_{k+1-j} \\ &= \frac{1}{T_s^N}\left[x_{k+1} + \sum_{j=1}^{k+1}(-1)^j \binom{N}{j} x_{k+1-j}\right] \end{aligned} \tag{19}$$

so

$$\begin{aligned} x_{k+1} &= T_s^N \Delta^{n} x_{k+1} - \sum_{j=1}^{k+1}(-1)^j \binom{N}{j} x_{k+1-j} \\ &= T_s^N A\cdot x_k + T_s^N B\cdot I_k + T_s^N \omega_k - \sum_{j=1}^{k+1}(-1)^j \binom{N}{j} x_{k+1-j} \end{aligned} \tag{20}$$

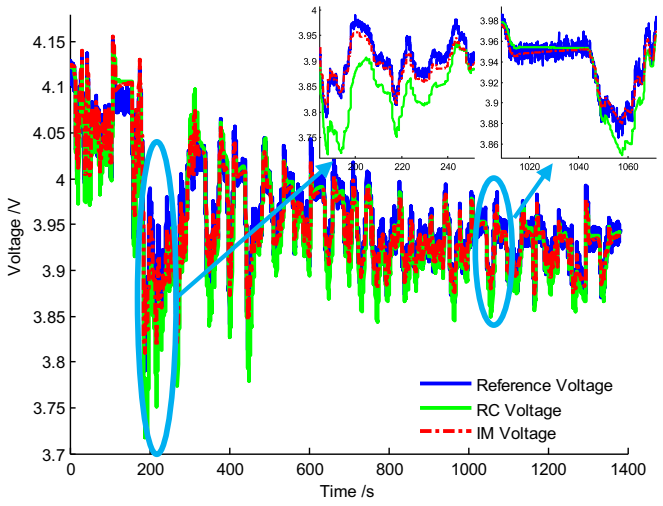

Fig. 6. Voltage response of the two model applied in a UDDS drive cycle.

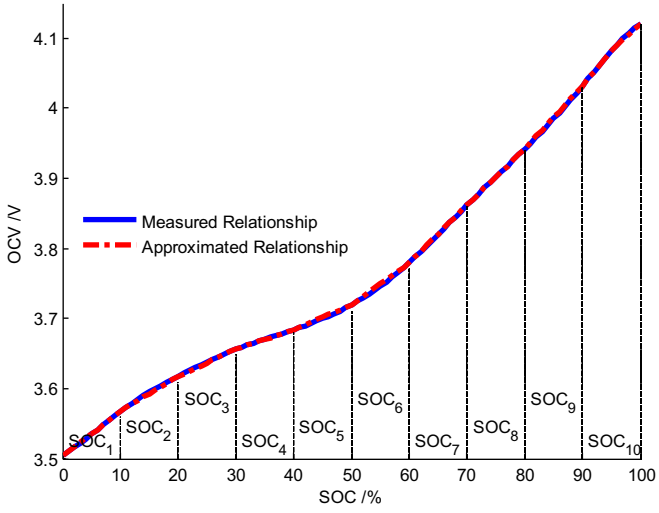

Fig. 7. Approximation of the relationship between SOC and OCV.

Table 2
Parameters of the approximation of the relationship between SOC and OCV.

*i*th	1	2	3	4	5	6	7	8	9	10
SOC_i	0–10	10–20	20–30	30–40	40–50	50–60	60–70	70–80	80–90	90–100
k_i	0.0059	0.0049	0.0039	0.0028	0.0036	0.006	0.0082	0.008	0.009	0.0099
b_i	3.5052	3.5188	3.5397	3.5728	3.5416	3.4199	3.2864	3.3004	3.2232	3.1364

The discrete state space function of the impedance model can be written as:

$$\begin{cases} x_{k+1} = T_s^N A x_k + T_s^N B I_k + T_s^N \omega_k - \sum_{j=1}^{k+1} (-1)^j \gamma_j x_{k+1-j} \\ y_k = C x_k + D I_k + v_k \end{cases} \quad (21)$$

where $\gamma_j = \binom{N}{j} = diag\left[\binom{\beta}{j}\binom{\alpha}{j}\binom{1}{j}\right]$.

The procedure of the state estimation of the fractional model of the Li-ion battery is as follows [21,23]:

for $k = 0$, the initial conditions is $x_0 \in R^3$, $P_0 = E[(\hat{x}_0^- - x_0)(\hat{x}_0^- - x_0)^T]$
for $k = 1, 2, \ldots$ compute:

State estimate time update:

$$\hat{x}_k^- = \Delta^N \hat{x}_k^- - \sum_{j=1}^{k} (-1)^j \gamma_j \hat{x}_{k-j}^+ = T_s^N A \hat{x}_{k-1}^+ + T_s^N B u_{k-1} - \sum_{j=1}^{k} (-1)^j \gamma_j \hat{x}_{k-j}^+ \quad (22)$$

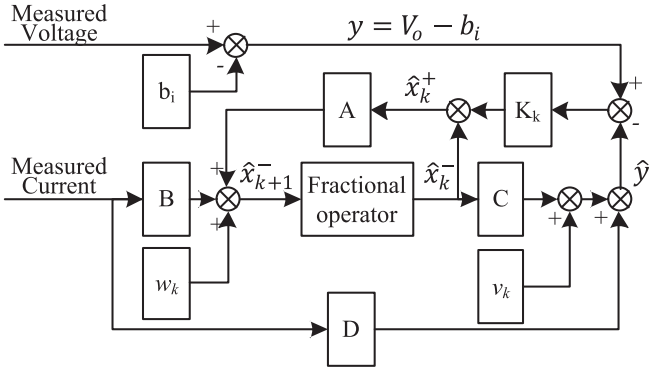

Fig. 8. Block diagram for the structure of fractional Kalman filter.

Error covariance time update:

$$\hat{P}_k^- = \left(T_s^N A + \gamma_1\right)\hat{P}_{k-1}^+\left(T_s^N A + \gamma_1\right)^T + Q_{k-1} + \sum_{j=2}^{k} \gamma_j P_{k-j} \gamma_j^T \quad (23)$$

Kalman gain matrix:

$$K_k = \hat{P}_k^- C^T \left(C \hat{P}_k^- C^T + R_k\right)^{-1} \quad (24)$$

State estimate measurement update:

$$\hat{x}_k^+ = \hat{x}_k^- + K_k(y_k - C\hat{x}_k^- - D I_k) \quad (25)$$

Error covariance measure update:

$$\hat{P}_k^+ = (I - K_k C)\hat{P}_k^- \quad (26)$$

where $Q_k = E[ww^T]$, $R_k = E[vv^T]$. The values for P_0, Q_k and R_k are difficult to determine, thus these parameters are selected by trial and error basis.

As far as convergence of the estimation method is concerned, researchers have pointed out that if the system was controllable and observable, then everything converges and the stationary filter was asymptotically optimal [23,24]. The system explored in this paper meets this requirement, so the estimated SOC will converge to the true value.

From the analysis above, the procedure of estimation based on the impedance model with fractional Kalman filter is shown in Fig. 8, where K_k is calculated through (24). The model output $\hat{y}$ is controlled with respect to battery terminal voltage V_o. The deviation between calculated $\hat{y}$ and measured y is fed back with the coefficient K_k, thus estimated states $\hat{x}_k^+$ are obtained with new measured information. Since SOC is one of the states, a more accurate SOC is updated.

5. Experimental verification

To illustrate the validity of the proposed model, an experimental battery test bench is developed. A 20 Ah Li-ion battery with Li $[NiCoMn]O_2$ based cathode and Graphite based anode is tested at

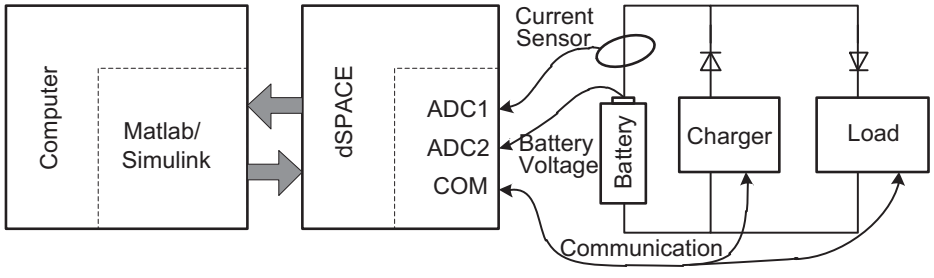

Fig. 9. Configuration of the battery experiment system.

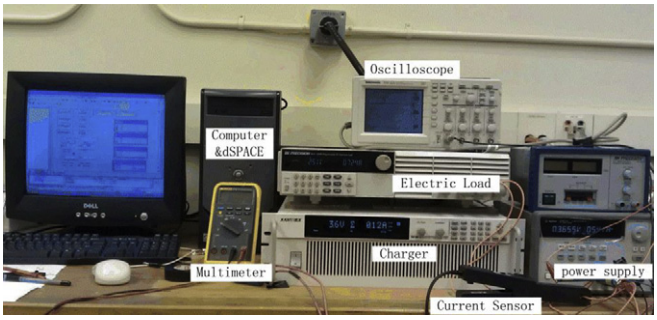

Fig. 10. Battery experiment workbench.

room temperature. The configuration of the battery experiment system is illustrated in Fig. 9. It consists of a computer in which a dSPACE 1104 board is installed. A charger and an electric load are connected in parallel with the battery through a diode separately as shown in Fig. 9. The charger and the electric load are controlled by dSPACE according to the signals given by the Simulink models. The current sensor measures the current flowing through the battery and reads it as voltage signals. These voltage signals together with the voltage of the battery are measured by dSPACE and fed back to the Simulink models. The battery experiment workbench is depicted in Fig. 10.

A UDDS drive cycle is applied to the battery. The magnitude of the current profile has been scaled down with respect to the battery features. The current profile of the UDDS drive cycle is given in Fig. 11. In the experiment, the terminal voltage and the current are measured and the current counting method is utilized to calculate the SOC as a reference. Since the initial SOC is known in the experiment and the experiment is relatively short term, the reference obtained by the coulomb counting method is considered to be the true SOC in this paper.

Since the actual initial states are difficult to know, P_0 is a given matrix in this paper, according to the definition of the states x, as $P_0 = \begin{bmatrix} 1 & 1 & 10 \\ 1 & 1 & 10 \\ 10 & 10 & 100 \end{bmatrix}$ for both IM estimator and RC estimator. Q_k and R_k are assumed to maintain constant during the estimation. However, these covariance values cannot be precisely known. So $R_k = 0.000001$ is selected for both the IM estimator and the RC estimator, while $Q_k = \begin{bmatrix} 0.0001 & 0.0001 & 0.003 \\ 0.0001 & 0.0001 & 0.003 \\ 0.003 & 0.003 & 0.09 \end{bmatrix}$ for the IM estimator, and $Q_k = \begin{bmatrix} 0.0001 & 0.0001 & 0.01 \\ 0.0001 & 0.0001 & 0.01 \\ 0.01 & 0.01 & 1 \end{bmatrix}$ for the RC estimator.

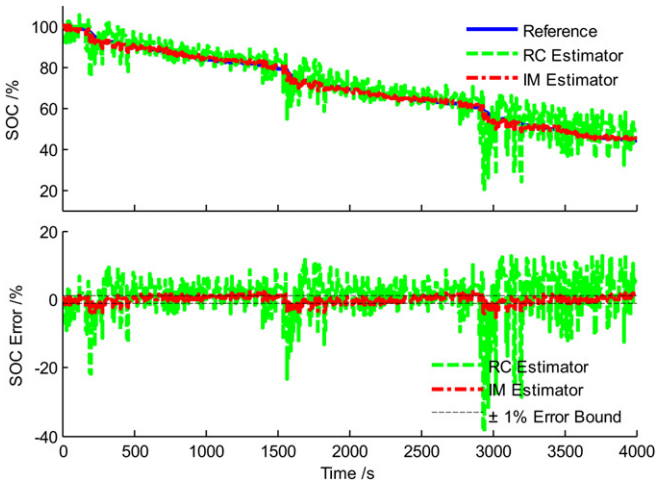

Fig. 12. SOC estimation results of the two estimators with known initial SOC.

In the first case, the initial state of the estimator is assumed to be known, which means the initial SOC is given. The results are shown in Fig. 12. And, the RC model is applied to compare the performance. To simplify the statement, the proposed estimate method based on the impedance model is referred to as an IM estimator, and the estimate method based on the RC model is referred to as a RC estimator.

As shown in Fig. 12, the two estimators can both trace the reference SOC, but with different accuracy. The ripples of the RC estimator are much bigger than those of the IM estimator. To show more details about the errors of the two estimators, the estimation errors are also depicted in Fig. 12. The curve of the IM estimator errors is almost a straight line near zero, mostly in the ±1% bound. To the contrary, the RC estimator errors vary a lot, with large error range, which could be more than 30%. The error distribution of the two estimators is given in Fig. 13. The error distribution for the IM

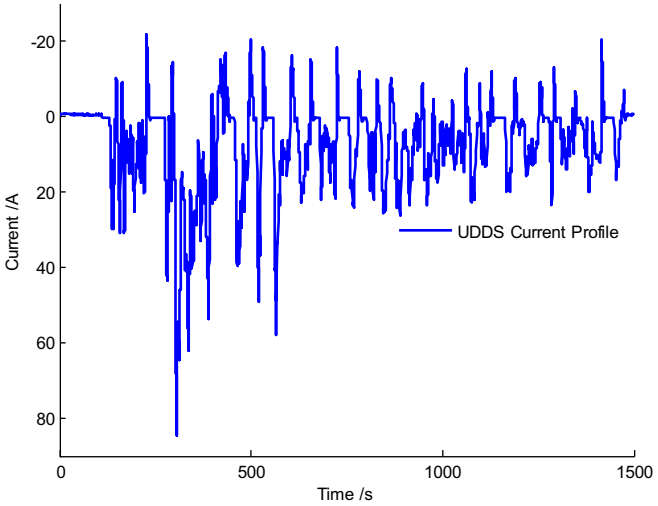

Fig. 11. The UDDS current profile.

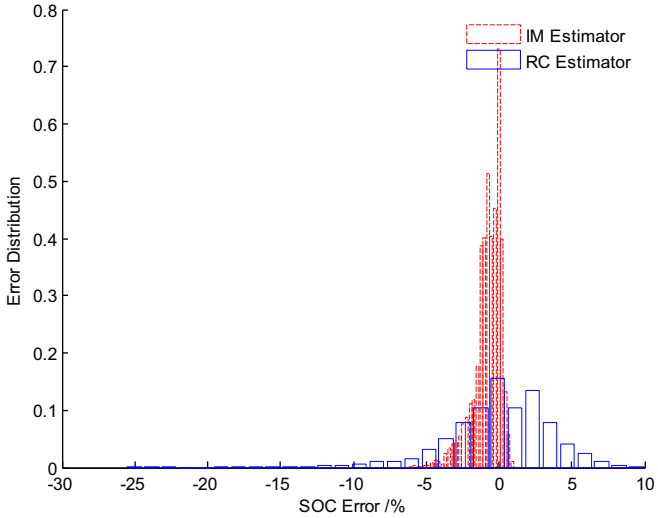

Fig. 13. The distribution of the estimation errors.

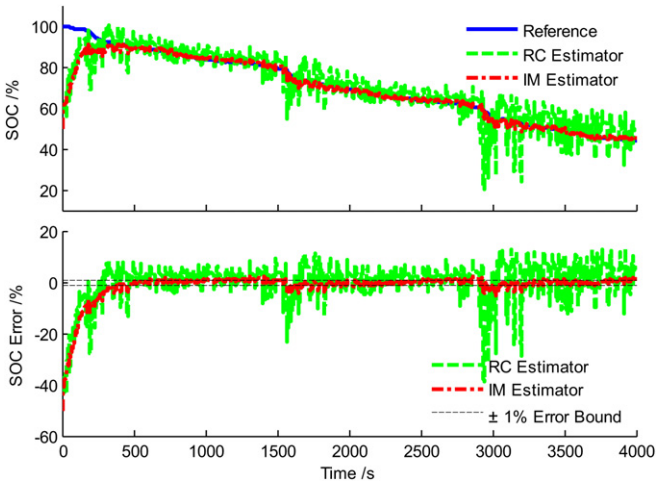

Fig. 14. SOC estimation results of the two estimators without known initial SOC.

estimator is narrower and more focused to the zero error section, indicating that the IM estimator has less estimation error and outperforms the RC estimator when the initial SOC is given.

In the second case, it is assumed that the initial SOC state is unknown, which means there would be an initial SOC error at first. The estimation results are shown in Fig. 14. The figure indicates that the two estimators can both converge to the reference SOC, but also with different accuracy. The proposed IM estimator converges to the reference SOC quickly, without overshoot or oscillation. And when it comes to the stable section, the trajectory of the IM estimator is always confined to the reference SOC with a small error mostly in the ±1% error band when it converges to the stable section, while the RC estimator gives much larger error.

6. Conclusion

This paper analyzed the impedance spectra of a Li-ion battery, and derived a simplified impedance model for the battery for the purpose of SOC estimations. To utilize such an impedance model to estimate the SOC of the battery, a FOC modeling method was introduced, interpreted in the form of FOC. A new identification methodology has been proposed which fully takes advantage of the properties of the impedance spectra and those of FOC.

The fractional Kalman filter was introduced to estimate the SOC based on the impedance model. To verify the performance of the proposed method, a battery experiment workbench has been developed. The results show that the proposed estimation method based on the impedance model outperforms that based on the RC model. The estimated SOC of the proposed method can quickly converge to the reference SOC and trace it well with a small error confined to ±1%.

References

[1] G.L. Plett, Journal of Power Sources 134 (2004) 262–276.
[2] V.H. Johnson, Journal of Power Sources 110 (2002) 321–329.
[3] H. He, R. Xiong, J. Fan, Energies 4 (2011) 582–598.
[4] K.M. Tsang, L. Sun, W.L. Chan, Energy Conversion and Management 51 (2010) 2857–2862.
[5] Y.H. Chiang, W.Y. Sean, J.C. Ke, Journal of Power Sources 196 (2011) 3921–3932.
[6] H. Hongwen, X. Rui, Z. Xiaowei, S. Fengchun, F. JinXin, IEEE Transactions on Vehicular Technology 60 (2011) 1461–1469.
[7] P. Mauracher, E. Karden, Journal of Power Sources 67 (1997) 69–84.
[8] S. Buller, E. Karden, D. Kok, R.W. De Doncker, IEEE Transactions on Industry Applications 38 (2002) 1622–1626.
[9] S. Buller, Impedance-Based Simulation Models for Energy Storage Devices in Advanced Automotive Power Systems, RWTH Aachen University, 2002.
[10] C. Min, G.A. Rincon-Mora, IEEE Transactions on Energy Conversion 21 (2006) 504–511.
[11] A. Hammouche, E. Karden, R.W. De Doncker, Journal of Power Sources 127 (2004) 105–111.
[12] I. Petráš, Fractional-order Nonlinear Systems: Modeling, Analysis and Simulation, Springer Verlag, 2011.
[13] C.A. Monje, Y.Q. Chen, B.M. Vinagre, D. Xue, V. Feliu, Fractional-order Systems and Controls: Fundamentals and Applications, Springer, 2010.
[14] J.A.T. Machado, A. Galhano, Journal of Computational and Nonlinear Dynamics 3 (2008) 021201–021205.
[15] J. Xu, J. Cao, B. Cao, Y. Li, Journal of Xi'an Jiaotong University 45 (2011).
[16] X. Yang, M. Liao, J. Chen, Procedia Engineering 29 (2012) 2950–2954.
[17] I. Sadli, M. Urbain, M. Hinaje, J.-P. Martin, S. Raël, B. Davat, Energy Conversion and Management 51 (2010) 2993–2999.
[18] J. Sabatier, M. Cugnet, S. Laruelle, S. Grugeon, B. Sahut, A. Oustaloup, J.M. Tarascon, Communications in Nonlinear Science and Numerical Simulation 15 (2010) 1308–1317.
[19] E. Karden, S. Buller, R.W. De Doncker, Journal of Power Sources 85 (2000) 72–78.
[20] J.R. McDonald, Impedance Spectroscopy: Emphasizing Solid Materials and Systems, Wiley-Interscience, 1987.
[21] D. Sierociuk, A. Dzieliński, International Journal of Applied Mathematics and Computer Science 16 (2006) 129–140.
[22] D.J. Leith, W.E. Leithead, International Journal of Control 73 (2000) 1001–1025.
[23] G.L. Plett, Journal of Power Sources 134 (2004) 252–261.
[24] J. Walrand, A. Dimakis, Random Processes in Systems – Lecture Notes (2006).